ELSEVIER

Journal of Nuclear Materials 294 (2001) 39–44

journal of nuclear materials

www.elsevier.nl/locate/jnucmat

Fission gas release and volume diffusion enthalpy in UO_2 irradiated at low and high burnup

J.P. Hiernaut *, C. Ronchi

European Commission Institute for Transuranium Elements, Karlsruhe, Germany

Abstract

Samples of UO_2, irradiated in LWRs at burnups from 25 000 to 95 000 MWd/t at in-pile temperatures below 800 K, were submitted to Knudsen-effusion experiments. In addition to the equilibrium vapour pressure of non-volatile species, release of fission gas was measured as a function of temperature and time up to approximately 2700 K, where complete vaporisation of the sample was eventually achieved. The fractional release curves of the main isotopes of Kr and Xe were measured and analysed with an algorithm adequate to discriminate between the relevant release stages, one of which, controlled by atomic diffusion, is analysed in this paper. The obtained enthalpy of diffusion – the same for all the examined nuclides – decreases from 4.6 eV/atom, at low burnup, to 2.95 eV/atom, at the highest burnup. Furthermore, the fraction of fission gas released via atomic diffusion markedly increases with increasing burnup, indicating a dramatic attenuation of the intragranular sink strength.

1. Introduction

Fission gas (FG) release in common nuclear reactors is produced by atomic diffusion in the oxide fuel, in conjunction with changes in morphology of its sintered and microscopic structure during irradiation. The process is in part ruled by events of stochastic nature. Consequently, whilst the overall FG release rate in a reactor operating at constant power is sufficiently reproducible, laboratory measurements performed on small samples, despite more controlled experimental conditions, are subjected to a much larger uncertainty. On the other hand, the aim of the analysis of laboratory experiments should be to provide a reasonable agreement at least on the fundamental quantities representing the mobility of atomic xenon and krypton in the crystal lattice of the fuel. Yet, even in front of this basic question, difficulties are encountered in the definition of a thermally activated diffusion coefficient, D, for almost insoluble gas-in-solid. The first difficulty regards the interpretation of the specific diffusion process investigated: whatever the measurement method of D may be, the occurrence of gas bubble precipitation affects the pre-exponential factor of the apparent diffusion coefficient. Correction for this effect requires a reassessment of the variable topology of the diffusion domain, which is not straightforward. Secondly, the FG in the lattice must be associated to a distinct free energy, [1] representing the reference state for the thermal activation of all atomic jumps. Whilst for soluble species this state is defined by measurable chemical potentials, for Xe and Kr this is merely dependent on the lattice strains around the inert atoms, whose evaluation can only be obtained by theoretical calculations.

* Corresponding author. Tel.: +49-7247 951 385 fax: +49-7247 951 198.

E-mail address: hiernaut@itu.fzk.de (J.P. Hiernaut).

[1] ... *a distinct free energy*: Actually gas-in-solid is a thermodynamic phase, i.e., a compound of gas and solid, whose free energy includes both short- and long-range interactions. Therefore, for a given temperature and pressure, only one distinct equilibrium configuration must be stable. However, most gas diffusion measurements are carried out under conditions very far from equilibrium, where gas atoms, at concentrations exceeding by orders of magnitude the solubility limit, may create different kinds of lattice defects and interact with them. Thus, in certain cases, the measured diffusion coefficient, D, may pertain to a phase in a non-identified, variable state. This obviously entails complications both in the experiment analysis and in the definition of D.

0022-3115/01/$ - see front matter
PII: S0022-3115(01)00469-X

In the investigation of FG diffusion in high burnup nuclear fuel, these interpretation problems are magnified. Comprehensive and accurate experimental data on FG release, though not sufficient to provide unambiguous answers to these questions, make it possible to obtain a self-consistent picture of the irradiation effects on FG diffusion.

Due to extension limits, this paper presents only partial results of a number of FG release experiments carried out at the European Institute for Transuranium Elements on LWR fuel irradiated from low to high burnups under different conditions. The subject will be therefore resumed in a following, more detailed article.

2. Experiment

2.1. Set-up

UO_2 samples, irradiated at various burnups, have been submitted to FG release experiments in a Knudsen-cell apparatus. Release was measured by mass spectrometry (MS) in a ultra-high vacuo, together with the effusion of volatile and less volatile fission products (the mass spectrometer was placed at a distance of a few centimetres from the sample, which was heated in a tungsten cell). Annealing tests were performed up to temperatures at which the sample completely vaporised. In conjunction with MS measurements, the FG escaping from the sample was collected in a liquid-nitrogen trap, where ^{85}Kr was measured by a counter, providing a check of the MS calibration constant for this gas. Furthermore, a flow β-counter, placed at the convergence of the outlet of the turbo-molecular pumps, provided an additional detection of ^{85}Kr slightly delayed with respect to that of the MS.

2.2. Sample characterisation

The samples investigated, in the form of a few chips of 10–20 mg total weight, were extracted from outer zones of commercial LWR rods that had been irradiated at temperatures below 700–800 K. For comparative purposes, samples that had experienced higher in-pile temperatures were also taken from different radial zones of pellet cross-sections and tested for FG release under the same conditions.

The state of the fuel (originally consisting of UO_2 pellets sintered to 95% of the theoretical density, with an average grain sizes of approximately 10 μm) was investigated both at irradiation end-of-life (EOL) and after laboratory thermal annealing. The results relevant for this context can be summarised as follows:

- Determination of the local burnup, in conjunction with FG content analysis, indicates that: (i) up to approximately 60 000 MWd/t almost all FG created was retained in the samples; whilst (ii) at higher burnups in-pile release progressively increased until approximately 10–15% of the inventory at 95 000 MWd/t.
- At low and moderate burnups, the FG was in part frozen in solution in the lattice and in part precipitated in the form of very heterogeneously distributed intragranular bubbles (with average sizes of 5–6 nm and concentrations of the order of magnitude of 10^{16} cm^{-3}). From the bubble size distribution, measured by transmission electron microscopy (TEM), the lower bound of the amount of FG precipitated in these bubbles at EOL is estimated to be of the order of 10–20% of the inventory.
- At burnups above 60 000 MWd/t, the samples increasingly exhibit the typical RIM re-structuring, consisting in build-up of sub-grains of approximately 0.1 μm in size. TEM observation [1] of these subgrains before and after laboratory thermal annealing shows that they contain a large amount of FG, part of which is in very small bubbles (<3 nm). These were observed to grow markedly after thermal annealing at 1300 K for 1 h (i.e. under conditions where onset of FG release is detected), with their concentration decreasing by approximately a factor of four.
- The concentration of retained FG in the RIM zone is still a matter of controversy. Actually, in LWR rods at high burnup, EMPA local measurements at different pellet radial positions show a marked fall of the xenon signal in the RIM zone [2]; this may be interpreted as a decrease of the local FG concentration. However, this conclusion is in some cases contradicted by XFR measurements on the same samples, which indicate in this zone an almost complete retention of Xe (see e.g. [3,4]). Very likely, the XFR measurements provide the correct concentration values, and hence EMPA needs probably major calibration adjustments for quantitative FG measurements in the RIM zone. In this work, five different samples were examined, which underwent in-pile RIM restructuring: MS measurements of the retained absolute amount of all major Xe and Kr isotopes provide evidence that *no dramatic in-pile release took place either during or after formation of the RIM structure.* Furthermore, the finely dispersed FG bubbles observed at EOL in these samples were certainly submitted, during low temperature irradiation, to fission-fragment re-solution. One should expect that a large fraction of FG had been consequently kept in dynamical solution by energetic recoil collisions, since re-solution is a very rapid process compared to both FG creation and precipitation at low temperature [5].
- A dense population of black dots and small loops are formed after annealing at 1300 K. Most of these defects, whose inter-distances are of the order 10–30 nm, produce in TEM a strain contrast. Part of them can be recognised as dislocation loops, others are

probably coherent precipitates of solid fission products (FP).
- Finally, the equilibrium vapour partial pressures of the uranium-bearing species were measured in the range 1900–2300 K with a sufficient precision for deducing, from the ratios of $UO_3(g)$ and $UO(g)$ to $UO_2(g)$, the fuel oxygen potential. This was decreasing during annealing in vacuo; the observed variation corresponds, in pure UO_2, to a change of the O/U ratio from 2.00 to 1.98.

3. Analysis of the release data

3.1. Method

Typical results of FG release measurements at low and high burnup are shown in Fig. 1. The analysis of the data was performed by means of a rate-equation system [6,7], which describes the fractional release, F, during thermal annealing as a function of temperature, T, and time, t, in terms of combined diffusion/trapping processes based on a schematic representation of the fuel structure, i.e.

3.1.1. Fuel displaying normal structure

Three gas migration steps are accounted for: (I) diffusion and venting of gas located on grain boundaries and dislocation networks; (II) volume diffusion from the body to the grain boundaries and (III) release of FG previously trapped in almost immobile intragranular bubbles due to progressive sublimation of the sample.

The three processes are assumed to be thermally activated, and each one expressed in terms of a characteristic entropy and enthalpy (this hypothesis is probably a very crude one for the first mechanism, but the erratic character of this initial stage does not justify, at least in the present context, a more critical approach).

3.1.2. Fuel displaying RIM structure

An important aspect to be considered is the effective cell radius of the volume-diffusion domain of the FG in the typical high burnup RIM structure [8,9], where the presence of sub-grains may entail formation of additional gas sinks with respect to the low-burnup structure. Actually, in the RIM structures observed in this work, the average interdistance of the vented pores is one order of magnitude larger than the smallest cells, whose walls do not appear to act as preferential loci for larger bubbles. This is likely due to the fact that the residual compressive strain/stress field created by burnup, and partially relieved by RIM restructuring, is probably concentrated in these tight dislocation networks, which should not offer more advantageous conditions for bubble growth.

We have then tried to fit the experimental data with a more complex, 'four-stage' model, in which stage II is split into two sub-stages, A and B. Stage IIA (intragranular precipitation and trapping on sub-boundaries) is governed, like in the first model, by volume diffusion, whilst stage IIB corresponds to migration along the extended defects (dislocation networks or sub-boundaries) of the RIM structure to the nearest free surface; this sub-stage is assumed to depend on a different gas diffusion coefficient, the magnitude of which should be between the volume and the grain-boundary diffusion coefficient.

Thus, if the sizes of the grains and sub-grains are given, the fractional release function $F(T(t))$ depends on five unknown parameters: the two diffusion enthalpies

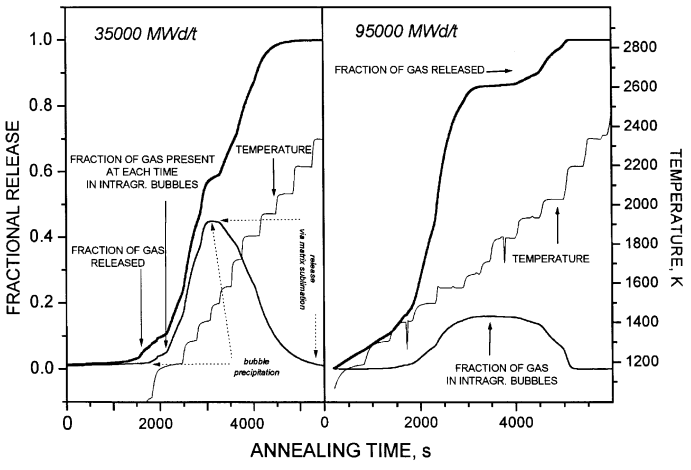

Fig. 1. Measured fractional release of ^{132}Xe at low and high burnup as a function of annealing time/temperature. The bell-shaped curves represent the current amount of gas precipitated into intragranular bubbles during annealing and subsequently escaped at higher temperatures through vaporisaton of the sample.

and three dimensionless constants depending on the product of the sink strengths considered (of bubbles, sub-boundaries and vented surface).

In both the adopted models, the fluxes of FG into interposed (bubbles, closed pores or extended defects) and open (free surface) sinks are described by a system of equations which, for laboratory annealing conditions, can be integrated analytically. The calculated convolution function, $Z(1/T(t))$, corresponding to the logarithm of the fractional rate of change of the FG retained in the sample, presents the following features: if the time scale of the thermal annealing is properly chosen, this function, independently of the annealing temperature history, $T(t)$, displays the various release stages as quasi-linear segments. These are connected by curves with minima that represent the increasing influence on release of FG trapping or exhaustion of venting processes. For customary fuel properties and increasing temperature programmes, function Z consists of segments defined by the sequence of the respective release-ruling mechanisms, i.e. gas diffusion along grain boundary (*straight line*); exhausting of vented pores (curve with minimum); diffusion from the grain (*straight line*), precipitation into intragranular bubbles (*curve with minimum*); vaporisation (*straight line*); exhausting of the sample by sublimation (*decreasing curve*). The shape of the entire curve $Z(1/T)$ depends on the competing sink strengths of the intragranular bubbles and of the grain boundary network, as well as on the rate of thermal annealing. Fig. 2 shows a typical curve calculated for optimal annealing conditions.

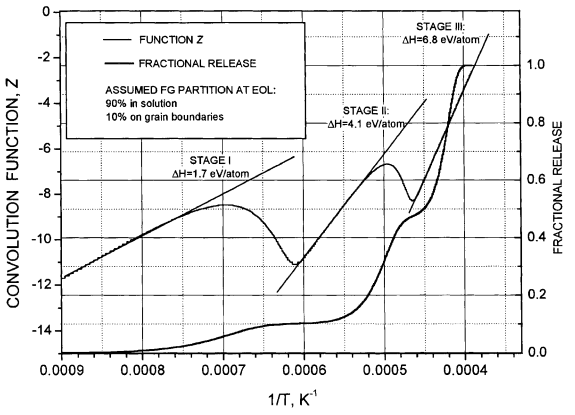

Fig. 2. Example of fractional release and related Z-curve as predicted by the 'three-stage'-model. The initial conditions correspond to a fission gas partition at EOL of 10% of the inventory on the grain boundaries and 90% frozen from dynamical solution. The annealing temperature is here assumed to increase linearly with time, and the calculation is cut before exhaustion of stage III.

If the T-independent constants of the rate equations are given, analysis of empirical release curves enables the amount of FG released in each stage to be evaluated, and, furthermore, provides both the activation enthalpy and the corresponding pre-exponential factor of the operating elementary diffusion process.

Fig. 3 shows function Z as measured in a high burnup sample. Obviously, a self-consistent identification of the different stages from empirical curves of FG release versus temperature/time cannot merely rely on the successful fitting of the model predictions. The model must be corroborated and proved sufficiently realistic for the analysis purposes. Thus, for stage III (matrix sublimation), the resulting enthalpy must be equal to the fuel vaporisation energy (≈6.72 eV/mol), and the pre-exponential factor must be near to that calculated from the equilibrium partial pressure of UO_2 for the given Knudsen-effusion conditions.

The features of stage II, examined in this work, are expected to depend principally on the enthalpy of diffusion of atomic gas. In fact, atomic diffusion controls the conflicting processes of gas migration to free surfaces and intragranular precipitation. The temperature/time conditions for the onset of stage II are mainly established by the enthalpy of activation, whilst its extent depends on fuel structure parameters (bubble size and concentration, grain size). Though, at a first sight, the analysis seems to be complicated, in practice, once stage III has been correctly identified, the variability of the diffusion enthalpy is limited, and stage II can be tracked down, from the onset of effective migration of gas to the

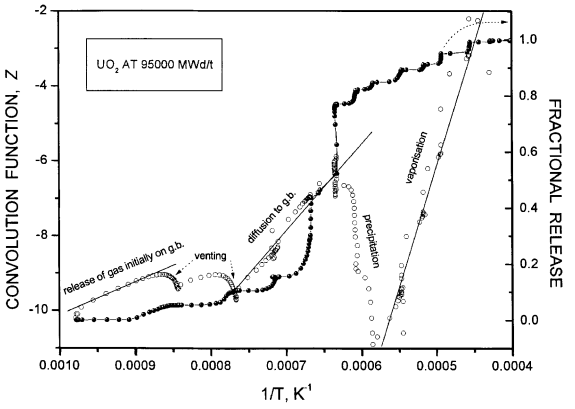

Fig. 3. Empirical function $Z(1/T)$ as measured in a sample of 90 000 MWd/t burnup and stepwise thermally annealed in laboratory. When the annealing conditions produce, as in the case illustrated, a Z-curve with well separated stages, numerical fitting of function $F(T,t)$ by the parameters of the three different release mechanisms leads to numerically stable results. The calculation of function Z during the transition stages controlled by venting or precipitation may be subjected to larger errors, introduced by numerical differentiation of the experimental (but also of the theoretical) values of F.

grain boundary up to completion of bubble precipitation.

Finally, under the reported experimental conditions, stage I takes place at temperatures at which the contributions of the other stages are negligible, and interests only the fraction of gas which had reached the grain boundaries during irradiation. Therefore, the results of the analysis of this stage do not affect those of the others. [2]

3.2. Result overview

All stable Xe isotopes were analysed together with ^{84}Kr and ^{86}Kr: their fractional release curves $F(T(t))$ are effectively equal. The volume diffusion enthalpies measured in fuels of different burnups are plotted in Fig. 4. Analysis of the FG release during laboratory annealing reveals that:

- *Stage I (involving gas migrated to the grain boundaries during reactor irradiation):* In samples irradiated at low temperatures (<800 K) less than 7% release is produced during this stage in low burnup samples; this fraction increases to approximately 15–20% at 95 000 MWd/t. Visual inspection of the sample during this stage reveals that at burnups above approximately 50 000 MWd/t this undergoes fine fragmentation as soon as the irradiation temperature is exceeded, i.e. much below the temperature at which massive release takes place. This confirms that most of the FG retained at EOL was finely dispersed in the fuel.
- *Stage IIA (involving long-range atomic diffusion of gas):* A clear shift towards lower temperatures of the onset of this stage was observed with increasing burnup. The deduced diffusion enthalpy decreases continuously from approximately 4.6 ± 0.13eV/atom, at 25 000 MWd/t burnup, down to approximately 3.47 ± 0.22 eV/atom at 60 000–70 000 MWd/t. If the 'three-stage' analysis is also applied to the release curves of higher burnups samples with RIM structure, the apparent enthalpy decreases further to 2.95 eV/atom.
- *Stage IIB (involving long-range atomic diffusion of gas on RIM sub-boundaries):* Such a fitting was made and the results are reported in Table 1. Though the uncertainty is larger than with the first model the following conclusions can be drawn:

  (a) If ordinary volume diffusion is supposed to occur only within the small ($\approx$0.1 μm) RIM cells, the resulting volume diffusion enthalpy, ΔH_{IIA}, is larger by $\approx$10–15% than that predicted by the first model; however, it still decreases with increasing burnup.

  (b) The resulting gas diffusion enthalpy on extended defects, ΔH_{IIB}, is closer than ΔH_{IIA}, to the average enthalpy obtained from the first model.

  (c) Finally, if the analysis is applied to release curves at low burnup – where a subgranular structure is only occasionally observed in the sample – the two enthalpies ΔH_{IIA}, and ΔH_{IIB}, converge, indicating that the diffusion rates in the two – in this case fictitious – diffusion domains must be effectively equivalent.
- *Stage III (involving release via matrix sublimation)*: Analysis of the data leads to the conclusion that the fraction of FG inventory precipitated into intragranular bubbles and released via sublimation decreased with burnup, while that diffusing to the free surface after escaping intragranular precipitation increased.
- *Gas trapping in bubbles:* As long as the as-fabricated sintered structure was maintained, the total amount of FG trapped in intragranular bubbles during thermal annealing was almost independent of burnup; whilst in the two samples with preponderant RIM structure, this amount was significantly lower.
- *In high burnup samples irradiated at higher temperatures*, the observed decrease in diffusion enthalpy was less pronounced. Moreover, the fraction of FG retained at EOL and precipitated in bubbles during laboratory annealing was much larger than in samples irradiated at in-pile temperatures below 800 K. This means that, in both respects, the effect of burnup in the former samples is significantly attenuated.

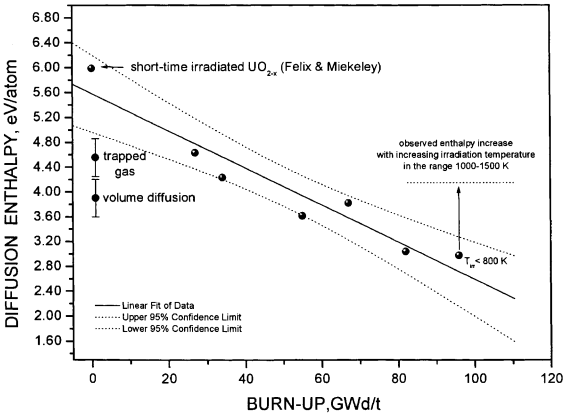

Fig. 4. Measured diffusion enthalpy of Xe and Kr in hypostoichiometric irradiated fuel as a function of burnup. The arrow at the right-hand-side indicates approximately the values obtained in samples of 95 000–100 000 MWd/t irradiated at higher temperatures.

A number of questions are posed by these results, regarding the effect of reactor irradiation on the atomic mobility of fission gas. The assumed release scheme,

[2] ... *do not affect those of the others:* However, the presence of release stage I may produce spurious diffusion coefficients if a simplistic analysis is used.

Table 1
FG diffusion enthalpy deduced from analysis of release data with, respectively, a 'three-stage' and a 'four-stage' diffusion model

Burnup (MWd/t)	First model stage II	Second model split stage II	
	ΔH_{II} : Migration within the grain (eV/atom)	ΔH_{IIA} : Migration within the subgrain (eV/atom)	ΔH_{IIB} : Migration on extended (eV/atom)
25 000	4.63 ± 0.04[a]	4.56 ± 0.2[b]	4.56 ± 0.2
50 000	3.61 ± 0.04	4.25 ± 0.2	3.73 ± 0.2
80 000	3.04 ± 0.04	3.56 ± 0.2	3.12 ± 0.2
95 000	2.97 ± 0.04	3.64 ± 0.2	3.04 ± 0.2

[a] The reported errors correspond to the fitting uncertainty of one single curve $F(t)$. Data on enthalpy accuracy are given in the text.
[b] Fictitious result, for substructure is completely absent in this sample.

based on precipitation/long-range migration/pore venting mechanisms seems to provide an explanation of the empirical data only up to moderate burnups.

For samples where the RIM structure becomes predominant, the experimental results may indicate an effective diffusion path where FG is first trapped on the observed sub-boundaries, and thereafter diffuses more effectively along the intricate network of extended defects, until it eventually reaches a free surface. However, in the absence of a precise, independent assessment of the effect of burnup on the volume diffusion enthalpy, this can be only regarded as a reasonable hypothesis.

4. Conclusions

Knudsen effusion measurements were carried out on UO_2 irradiated at different burnups until complete vaporisation of the sample. The analysis of FG release as a function of temperature was carried out with an algorithm that enables the rate-controlling mechanisms to be recognised, i.e. nondescript venting processes of grain-boundary porosity, gas volume-diffusion, and sublimation of the matrix. The second stage was analysed in this paper, and the following results were obtained:

– The enthalpies of diffusion of all Kr and Xe isotopes are effectively equal and, within the experimental error, decrease linearly with increasing burnup from 4.6 to 2.95 eV/atom. The intercept at zero burnup (5.64 eV/mol) is near to a literature value measured in hypostoichiometric single crystals of uranium dioxide (6.0 eV/atom) [10].

– Furthermore, at the highest burnup (95 000 MWd/t) the FG amount reaching the free surfaces (without being captured by intragranular bubbles) is four times larger than at low burnup (25 000 MWd/t). This effect is most intriguing, since it contradicts the predictions of gas precipitation models based on random-walk precipitation.

– Finally, the effect on FG release of the typical submicroscopic RIM structure formed at high burnup was investigated. The sub-grain walls were supposed to represent pathways for long-range migration of FG rather than deep sinks for bubble precipitation. This 'four-stages' diffusion model provides a reasonable agreement with the experimental data.

References

[1] I. Ray, H. Thiele, European Institute for Transuranium Elements, Karlsruhe, (Germany), unpublished results.
[2] C.T. Walker, J. Nucl. Mater. 375 (1999) 56.
[3] M.E. Cunningham, M.D. Freshley, D.D. Lanning, J. Nucl. Mater. 188 (1992) 19.
[4] M. Mogensen, J.H. Pearce, C.T. Walker, J. Nucl. Mater. 264 (1999) 99.
[5] R.S. Nelson, J. Nucl. Mater. 31 (1969) 153.
[6] F. Capone, J.P. Hiernaut, M. Martellenghi, C. Ronchi, Nucl. Sci. Eng. 124 (1996) 436.
[7] C. Syros, I. Sakellaridis, C. Ronchi, J. Nucl. Mater. 168 (1989) 65.
[8] J. Spino, K. Vennix, M. Coquerelle, J. Nucl. Mater. 231 (1996) 179.
[9] J. Spino, D. Baron, M. Coquerelle, A.D. Stalios, J. Nucl. Mater. 256 (1998) 189.
[10] W. Miekeley, F.W. Felix, J. Nucl. Mater. 42 (1972) 297.